Electrochemical Studies on the Growth Process of the Zinc Oxide Films from Nitrate Solutions

CLAUDIA SORINA DUMITRU[1], MARIANA SIMA[2], ANCA COJOCARU[1]*

[1]University POLITEHNICA of Bucharest, Faculty of Applied Chemistry and Materials Science, 132 Calea Grivitei, 010737, Bucharest, Romania

[2]National Institute of Materials Physics, P.O. Box MG 7, 077125 Magurele, Romania

The cathodic deposition of zinc oxide film on Pt from an aqueous solution containing 0.05 M $Zn(NO_3)_2$ was investigated using linear sweep voltammetry and electrochemical impedance spectroscopy. The film formation is an electroprecipitation process due to reduction of nitrate ion on the surface of working electrode in the presence of Zn^{2+} ions. A morphology of ZnO with hexagonal platelets was observed. The standard electromotive force of the cell reaction was calculated for both NO_3^-/NO_2^- process and overall deposition process. Linear voltammograms and visual observations showed that polarizing the electrode at higher negative potentials than -1.1 V, the parallel reduction of zinc ion to zinc metal occurs together with reduction of nitrate ion to hydroxide ion; as a consequence, a partial amorphous state of ZnO film was recorded on SEM micrographs. Experimental impedance data and data calculated by fitting with an equivalent circuit showed that the ZnO formation involves an adsorption of complexed zinc ions on Pt electrode, before the charge transfer.

Keywords: zinc oxide, zinc nitrate electrolyte, electrodeposition, linear sweep voltammetry, electrochemical impedance spectroscopy

Being a material with remarkable and unique optical and electronic properties zinc oxide (ZnO) has attracted a lot of research interest in recent years. Due to its wide band gap (3.36 eV), it is transparent in the visible radiation. In addition, ZnO is a piezoelectric material, has a great magneto-optical effect, and behaves as a good chemical sensor. Deposition of zinc oxide films has been studied by various techniques in order to obtain applications such as optoelectronic devices, transistors, UV photodiodes, light emitting diodes and laser diodes, gas sensors, ultrasonic oscillators and piezoelectric transducers [1]. Highly transparent conducting ZnO layers with anti-reflective properties are important components of photovoltaic solar devices and displays [2].

Recent techniques of ZnO deposition, such as chemical vapour deposition (CVD), metal-organic CVD (MOCVD), RF magnetron sputtering, spray-pyrolysis, molecular beam epitaxy, pulsed laser deposition, etc. allow obtaining high quality ZnO films. ZnO can also be grown by electrodeposition, which is simple to be operated, avoids the use of vacuum pumps and has low installation and production cost with minimum ambient impact. Electrodeposition has the advantage of low temperature processing, allows various substrate shapes and controllable film thickness. Also, it is interesting to note that the production of the zinc oxide semiconductor is direct, without the need for subsequent annealing.

The first studies regarding the electrochemical deposition of zinc oxide from nitrate aqueous solution were published by Izaki et al. [3,4], and then some investigations were reported, working usually with 0.1 M $Zn(NO_3)_2$ hot aqueous solution [5-9]. Otani et al. [7] have also studied the effect of bath temperature on the electrodeposition mechanism of ZnO; the film was prepared from 0.1 M zinc nitrate aqueous solution in potentiostatic conditions at 40-70^{0}C.

The mechanism of zinc oxide thin films prepared by electrodeposition from nitrate solution has been studied by Yoshida [6]. In general, the methods of zinc oxide electrodeposition in aqueous media are based on the generation of hydroxide ion (OH^-) on the electrode surface by cathodic reduction of a precursor in a solution with Zn^{2+} ions. Nitrate ion (NO_3^-) is here the precursor of OH^- formation. Zn^{2+} and OH^- ions react with each other and result in the deposition of ZnO on the cathode surface. Mahalingam et al. [10,11] have researched extensively the microstructure of electrodeposition zinc oxide thin films grown from nitrate solution. We recently obtained ZnO or ZnO doped nanowires by electrodeposition in pores of polycarbonates membranes using template method and nitrate solution [12-14]. Chander and Raychaudhuri [15] also showed that ZnO nanorods can be grown by electrodeposition from aqueous solution of zinc nitrate with hexamethylene tetramine addition.

The aim of this paper is the study of electrochemical deposition of zinc oxide from zinc nitrate aqueous solution by linear sweep voltammetry and electrochemical impedance spectroscopy.

Experimental part

The salt reagents $Zn(NO_3)_2.6\,H_2O$, $ZnSO_4$ and KNO_3 were purchased from Merck and used as received without purification. The solvent was bidistilled water. The electrochemical cell contained either a Pt foil (0.5 cm^2) or a Pt disk (3 mm diameter) as working electrodes, a pure zinc (99.9%) rod (4 cm^2) as auxiliary electrode and a saturated calomel electrode (SCE) or Ag,AgCl/KCl 3M as reference electrode. Measurements by both linear sweep voltammetry (LSV) and electrochemical impedance spectroscopy (EIS) were performed using a VOLTALAB 10 potentiostat digitally controlled by a PC computer. EIS tests were carried out in 10^{-2} Hz $\leq$ f $\leq$ 10^5 Hz frequency range

* *email: a_cojocaru@chim.upb.ro*

with an a.c. voltage amplitude of ± 5 mV, at a cathodic potential of -0.7 V/SCE and keeping constant temperature of the solutions at 70°C. The experimental impedance spectra were interpreted on the basis of equivalent electrical circuit using a specialized fitting software, Zview 2.90c.

ZnO thin films were electrodeposited potentiostatically on Pt substrate for different electrolysis times, using the same conventional three-electrode system and VOLTALAB 10 potentiostat/galvanostat. The aqueous solution contained 0.05 M zinc nitrate dissolved in bidistilled water. The temperature was maintained constant at 70°C. ZnO films with 0.5 cm^2 surface area were grown at various cathodic potentials between -0.900 and -1.300 V vs. SCE to study their aspect and properties. The microstructures of deposits were imaged with a Hitachi S-2600N SEM microscope equipped for chemical composition analysis with an energy dispersive X-ray analysis (EDX) device from Röntec GmbH.

Results and discussions

The electrochemical deposition of ZnO on the electrode surface is in fact a pure chemical sequence of Zn^{2+} ions precipitation as zinc hydroxide in the presence of electrochemically formed hydroxyde anions. Zinc hydroxide is a non-stable compound and converts rapidly, so that the resulted product in spontaneous dehydration is zinc oxide, ZnO:

$$Zn^{2+} + 2OH^- \rightarrow Zn(OH)_2 \rightarrow ZnO\downarrow + H_2O \quad (1)$$

Hydroxyde ions (OH^-), which act as the precursors for the formation of zinc hydroxide, can be electrochemically obtained in the nitrate solution *via* reduction of nitrate ion at the cathode:

$$NO_3^- + 2\,e^- + H_2O \rightarrow NO_2^- + 2OH^- \quad (E^0 = -0.250\ V/SCE) \quad (2)$$

Taking into account that there are various reduction processes of NO_3^- ions, to our opinion the most useful for ZnO deposition is this cathodic reaction (eq. (2)), because other processes of NO_3^- reduction produce gaseous compounds whose adsorption on the electrode can suppress growth of ZnO. It is worth to mention that another way to obtain hydroxyde species is by bubbling oxygen in aqueous solutions [16]. In this case, the electrochemical ZnO deposition involves also an initial step that corresponds to the formation of hydroxide ions by reduction of molecular oxygen:

$$O_2 + 4e^- + 2\,H_2O \rightarrow 4\,OH^- \quad (3)$$

This electrochemical process may occur also in aerated aqueous solutions. The obtained hydroxide ions increase the local *p*H on the electrode surface, so that the *p*H can reach even a value of 10 [3], determining the precipitation of $Zn(OH)_2$.

By summing up both processes (1) and (2), the total electrochemical reaction may be written as:

$$Zn^{2+} + NO_3^- + 2e^- \leftrightarrow ZnO\downarrow + NO_2^- \quad (E^0 = +0.246\ V/SCE) \quad (4)$$

The E^0 values (the electromotive force of the cell reaction under standard conditions) for the two reactions were calculated from standard Gibbs free energies of the corresponding reaction (ΔG^0) by considering the well-known equation:

$$\Delta G^0 = - z F E^0 \quad (5)$$

Values of ΔG^0 for electrochemical reactions (2) and (4) may be obtained from the Gibbs free energies of formation (ΔG_f^0) of individual chemical species in aqueous medium at 298 K. In the equation (5) z represents the number of electrons transferred, and F is the Faraday constant. The used ΔG_f^0 values of chemical species which participate in these reactions are listed in table 1 [17].

We calculated ΔG^0 = 1.68 kJ/mole for reaction (2) and ΔG^0 = -94.32 kJ/mole for reaction (4); by taking values of z = 2 and F=96487.3 C/equiv. and considering the potential of saturated calomel electrode (SCE) of +0.242 V/NHE, the resulted values of E^0, -0.250 V and +0.246 V were written near each equation, (2) or (4), respectively. This way of thermodynamic calculation is very useful, for interpretation the linear sweep voltammograms and processes.

Figure 1 shows the linear voltammograms of nitrate ion reduction on Pt foil electrode in the presence of either single potassium ion or both potassium and zinc ions. The continuous increase of current on curve (1) should be related to the reduction of NO_3^- species resulting hydroxide anions. Looking at curve (2) it can be observed the significant growth of reduction current in the solution containing zinc ions, the formed hydroxide ions being consumed on the electrode surface owing to zinc hydroxide precipitation, followed by ZnO formation. On curve (2) from figure 1, two reduction processes are observed. The first process is an increase of cathodic current starting with -0.25 V potential, which was assigned to reduction of nitrate ion from aqueous solution. The large peak with a maximum at around -1.35 V on curve (2) is due to a massive ZnO layer formation, zinc oxide precipitated film being a semiconductor which inserts in the circuit a supplementary ohmic resistance and causing a temporary current decrease. The second process starting at -1.4 V is assigned to hydrogen evolution and zinc deposition [3].

Comparative linear voltammograms exhibiting the differences in electrochemical precipitation of ZnO from

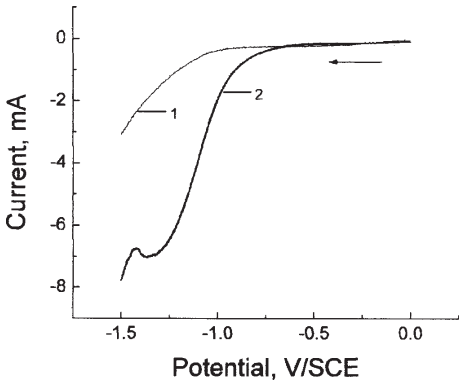

Fig. 1. Linear voltammograms on platinum electrode (0.5 cm^2) in two aqueous solutions: (1) 0.05 M KNO_3; (2) 0.05 M $Zn(NO_3)_2$; temperature 70°C, scan rate 5 mVs^{-1}

Species	NO_3^-	H_2O	NO_2^-	OH^-	Zn^{2+}	ZnO
ΔG_f^0, kJ/mole	-111.3	-237.14	-32.2	-157.28	-147.1	-320.52

Table 1
VALUES OF GIBBS FREE ENERGY OF FORMATION FOR VARIOUS SPECIES INVOLVED IN ZnO ELECTRODEPOSITION

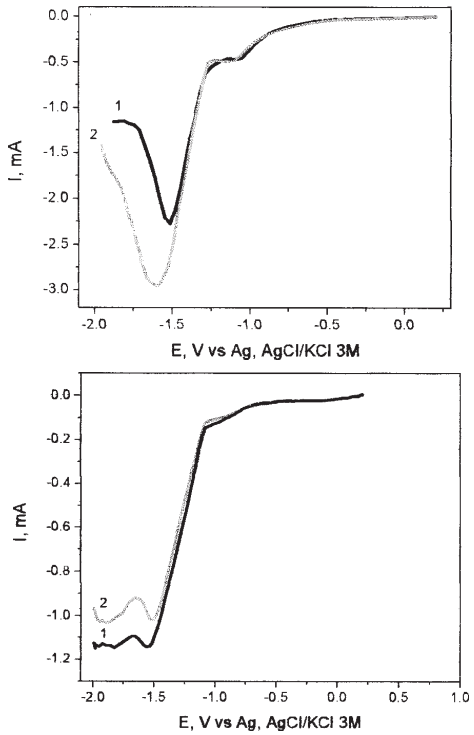

Fig. 2. Comparison of linear voltammograms on platinum disk electrode (0.07 cm^2) in aqueous solutions containing: (a) 0.05 M $Zn(NO_3)_2$; (b) 0.05 M $ZnSO_4$. Temperature 70^{0}C, scan rates: 50 mVs^{-1} (curves 1) and 100 mVs^{-1} (curves 2)

aqueous solutions containing either zinc nitrate or zinc sulfate are shown in figures 2. The molarities of Zn^{2+} ion in solution are similar, with a value of 0.05 M. However, as also figure 2a shows, we noticed that ZnO film is substantially obtained from zinc nitrate solution starting from -1.1 V as a first step, whereas a metallic zinc deposition occurs subsequently on platinum at a potential of -1.5 V (curve 1) or -1.6 V (curve 2). At potentials more negative than -1.9 V the hydrogen evolution takes place. In zinc sulfate solution, the metallic zinc deposition begins at potentials more negative than -0.7 V with a sudden increase of cathodic current at -1.1 V up to -1.4 V where the process of hydrogen evolution starts. The differences can be seen clearly by watching the appearance of platinum electrode immersed in nitrate solution. Within the time interval when the potential is scanned up to -1.1 V, or more negatively, it was found that both white ZnO film and dark grey metallic zinc clusters are deposited on the electrode surface. More interestingly, these clusters quickly change their colour which turns also in white, indicating a pure chemical oxidation process. This behaviour can be understood if we consider a simultaneous coupling of the zinc ion reduction and nitrate ion reduction (the last leading to hydroxide ion) and this coupling proceeds on the already deposit of crystalline zinc oxide. Using $ZnSO_4$ solution as electrolyte, the platinum is covered with metallic zinc, only.

During measurements made in the temperature range of 25-92^{0}C [18] we obtained linear voltammograms on Pt immersed in 0.05 M $Zn(NO_3)_2$ solution, at 5 mVs^{-1} scan rate (not shown), and we noticed that the ZnO deposition process takes place at a faster rate at higher temperatures. In the majority of cases, the cathodic potential at which the massive formation of ZnO film occurs was found to be –1.1 V (vs. SCE), confirmed the Mahalingam' foundings [10] from cyclic voltammetry studies. Temperature affects particularly the nitrate ion reduction process and ZnO

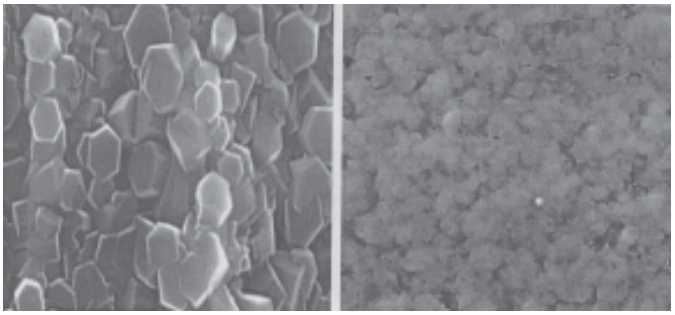

Fig. 3. SEM micrographs of ZnO film deposited on Pt electrode from 0.05 M $Zn(NO_3)_2$ solution, after 35 min. electrolysis at 70^{0}C temperature; the Pt electrode was polarized at constant potentials: (a) -0.7 V and (b) -1.2 V. Magnification: ×60000

precipitation, so that, practically, the ZnO formation process does not take place at a temperature below 45 ^{0}C.

Otani et al. [7] also showed that the ZnO film deposition depends strongly on bath temperature, because the mechanism involves an increased thermodynamic stability of ZnO at high temperature. Based on electrochemical quartz-crystal microbalance (EQCM) analysis, it was suggested that $Zn(OH)_2$, which is precursor of ZnO, is slowly converted in ZnO at low temperature, but the formation of ZnO is extremely rapid at high temperature. It was interpreted that ZnO directly deposits on substrate at high temperature.

Several coating experiments were carried out in zinc nitrate solutions with different intervals of electrolysis time and different temperatures (70-92^{0}C) in potentiostatic conditions. Uniform ZnO films were obtained under optimized conditions (potentials more negatively than -1.1 V). Many as-electrodeposited films were semitransparent but others were white; they were high adherent to the platinum substrate. The electrochemical deposits as ZnO thin films were in most cases polycrystalline, with grain size depending on experimental conditions.

Figures 3 present comparatively SEM images of ZnO films electrodeposited on Pt at two cathodic potentials, namely -0.7 V and -1.2 V. ZnO layers, showing compact, void-free surface, with a densely packed structure without pores are illustrated in both cases.

A hexagonal morphology is noticed, but a degree of disorder (and even a degree of amorphous state) is seen for ZnO film prepared at -1.2 V polarization compared with film obtained at -0.7 V. Such behaviour can suggest simultaneous co-deposition of both ZnO and zinc metal at -1.2 V potential and Zn clusters turn into amorphous ZnO, as indicated above. Figure 3a shows that most zinc oxide microcrystals deposited at -0.7 V have a shape of hexagonal platelets rather of hexagonal pillars (as indicated in some papers [16,19]).

The processes occurring at platinum electrode during deposition of zinc oxide film were also studied using electrochemical impedance spectroscopy. It should be noted that during the recording of the impedance diagram, ZnO clusters are generated and they are separated from each other; the following step is their growth onto electrode surface.

Figures 4 show the Nyquist and Bode spectra of Pt electrode polarized in 0.05 M $Zn(NO_3)_2$ solution at -0.7 V/SCE. Both representations suggest three time constants: the first is related to the behaviour of typical capacitive interface, electrolyte / Pt electrode, as a Nyquist semicircle with very small diameter, in high frequencies domain; the second one is related to the ZnO film forming stage (capacity and ohmic resistance of the film) and

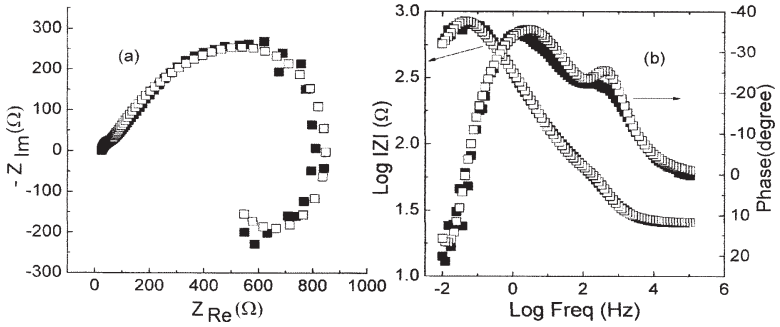

Fig. 4. Nyquist diagram (a) and Bode diagram (b) for Pt electrode (0.5 cm^2) polarized at -0.7 V/SCE in 0.05 M $Zn(NO_3)_2$ solution; ■■■ - experimental data; □□□ - the fitted data.The temperature was maintained constant at 70^0C

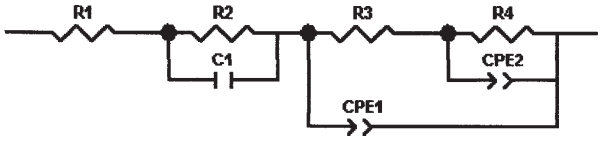

Fig. 5. Equivalent electrical circuit used for fitting the experimental data showed in figures 4

corresponds to a large Nyquist semicircle at intermediate frequencies; at frequencies below 1 Hz, Nyquist diagram shows a so-called "inductive behavior" (inductive loop) when the imaginary part of the impedance takes positive values. The last time constant was found usually in zinc electrodeposition processes [20,21] and has been attributed to adsorption onto electrode surface of various species existing in solution, before the electroreduction process. Actually, this electromagnetic induction phenomenon is not related to electrochemical process of ZnO deposition. Bode spectra (fig. 4b) show the same series of gradual modifications according to the existence of three time constants: the impedance modulus consists in three curved portions and the phase angle curve exhibits two maxima with values reaching approx. -40^0, a value which is characteristic for the diffusion through the formed film.

The results of impedance measurements performed in Pt/zinc nitrate solution system with frequencies within 10^5-0.01 Hz at -0.7 V polarization potential were fitted by the use of an equivalent electrical circuit (fig. 5) and ZView software. The simulated impedance curves (both Nyquist and Bode spectra) are also represented in figures 4.

The outer part of the interface is simulated by the part of circuit consisting in a combination of ohmic resistance of electrolyte solution (R1) in series with a parallel circuit which represents the first time constant; this parallel circuit contains the charge transfer resistance R2 for the electroreduction of nitrate ion in parallel with a capacitance C1 related to behaviour of electrical double layer. Next part of circuit is related to the second time constant representing the resistance and capacitance of formed ZnO film, respectively, and has as components the ohmic resistance R3 in parallel with a constant phase element CPE1. The third time constant is related to adsorption; the corresponding part of circuit contains the ohmic resistance R4 (which is in series with R3 resistance) in parallel with a second constant phase element CPE2.

In general, a constant phase element CPE illustrates the deviation from behaviour of an ideal capacitor [22,23]; CPE has as components CPE-T as a capacitance part and CPE-P as an exponent (P=1 for pure capacitance, P=0 for pure resistor and P=-1 for pure inductance). The impedance of CPE is defined by equation:

$$Z(CPE) = \frac{1}{T\,(i\omega)^P} \qquad (6)$$

with ω –the angular frequency and $i = \sqrt{-1}$

Table 2 contains the calculated values for the circuit elements for the best fitting of experimental data.

According to table 2, the ohmic resistance of electrolyte is R_s = 12.6 Ωcm^2 which is a plausible value for aqueous solution at 70^0C temperature. We also calculated the charge transfer resistance of electrochemical process (R_{ct} = 10.2 Ωcm^2) from the value of R2 component. R_{ct} is correlated with the exchange current density (i_0) by equation:

$$R_{ct} = \frac{RT}{zFi_0} \qquad (7)$$

where R, T and F have their usual significances. Taking z = 2, a value of i_0 = 1.27 $mAcm^{-2}$ was obtained at 70^0C temperature, which is of the same order of magnitude as those indicated in literature [24]. The capacity of the electrical double layer (C_{dl}) is correlated to value of C1 from table 2. The obtained value for Pt electrode/solution interface, 46.4 μFcm^{-2}, is a little bit higher than the C_{dl} values in the most aqueous electrolytes (15-30 μFcm^{-2}), suggesting a larger active surface area than the geometrical one. The ohmic resistance due to growing ZnO film (216.8 Ωcm^2 calculated from R3) is also higher than that expected; this may be explained by unstable intergranular contacts in aqueous medium.

A separate discussion may be made about the adsorption phenomenon and value of R4. It is difficult to directly reduce nitrate ions on the cathode due to electrostatic repulsion between them and this negatively polarized electrode. It was observed that nitrate ion reduction potential shifts toward more positive values in the presence of metal ions (Zn^{2+}) and it was assumed that

Table 2
VALUES OF COMPONENTS FOR THE EQUIVALENT ELECTRICAL CIRCUIT SIMULATING THE PROCESSES ON Pt ELECTRODE (0.5cm^2)IN 0.05 M $Zn(NO_3)_2$ SOLUTION POLARIZED AT -0.7 V/SCE POTENTIAL

Circuit parameter and measure units		Values for -0.7 V polarization
R1, Ω		25.2
R2, Ω		20.4
C1, μF		23.2
R3, Ω		433.6
R4, Ω		707.1
CPE1	T, Ω^{-1} s^P	9.1×10^{-4}
	P	0.56
CPE2	T, Ω^{-1} s^P	2.7×10^{-4}
	P	-1

this metal ion acts as an intermediary species in the process of charge transfer from the electrode to nitrate ion [25]. Also, the rate of process for electroreduction of nitrate ions is influenced by the stability of the complexes formed by hydrolysis of metal ions in the solution and their adsorption. Zinc ions are surrounded by a mixture of water molecules and a number of NO_3^- ions, thus influencing their adsorption on the electrode before the charge transfer. As shown from the data in table 2, the resistance of this adsorption process (353.6 Ωcm^2) is relatively high, indicating a rate determining step.

Conclusions

The electrochemical deposition of ZnO in zinc nitrate aqueous solution is an electroprecipitation process due to reduction of nitrate ion on the surface of working electrode in the presence of Zn^{2+} ions. ZnO films were grown on Pt starting from -0.7 V (*vs*. SCE). It was found that polarizing the electrode at higher negative potentials than -1.1 V, the reduction of zinc ion to zinc metal occurs simultaneous to reduction of nitrate ion to hydroxide ion. However, due to alkalinization of medium near the electrode surface, zinc particles convert rapidly into zinc oxide. From the impedance spectra it results that the overal electrochemical process has three time constants related to charge transfer, ZnO film formation and adsorption of zinc ions surrounded by both water molecules and nitrate ions, a slow process before the charge transfer.

Acknowledgements: Claudia Sorina Dumitru is grateful for financial support from the European Social Fund through POSDRU /88/ 1.5/S/ 60203 Project.

References

1. KIM, K.K., SONG, J.H., SONG, H.J., CHOI, W.K., PARK, S.J., SONG, J.H., J. Appl. Phys., 87 (7), 2000, p. 3573.
2. ILLY, B.N., CRUICKSHANK, A.C., SCHUMANN, S., DA CAMPO, R., JONES, T.S., HEUTZ, S., McLACHLAN, M.A., McCOMB, D.W., RILEY, D.J., RYAN, M.P., J. Mater. Chem., 21, 2011, p. 12949.
3. IZAKI, M., OMI, T., Appl. Phys. Lett., 68, 1996, p. 2439.
4. IZAKI, M., OMI, T., J. Electrochem. Soc., 143, 1996, p. L53.
5. DALCHIELE, E.A., GIORGI, P., MAROTTI, R.E., MARTIN, F., RAMOS-BARRADO, J.R., AYOUCI, R., LEINEN, D., Solar Energy Mater. Solar Cells, 70, 2001, p. 245.
6. YOSHIDA, T., KOMATSU, D., SHIMOKAWA, N., MINOURA, H., Thin Solid Films, 451–452, 2004, p. 166.
7. OTANI, S., KATAYAMA, J., UMEMOTO, H., MATSUOKA, M., J. Electrochem. Soc., 153 (8), 2006, p. C551.
8. PENG, F., LI, X.M., GAO, X.D., Key Eng. Mater., 336-338, 2007, p. 2221.
9. GEORGIEVA, V., TANUSEVSKI, A., AIP Conf. Proc., 899, 2007, p. 756.
10. MAHALINGAM, T., JOHN, V.S., HSU, L.S., J. New Mater. Electrochem. Syst., 10, 2007, p. 9.
11. MAHALINGAM, T., JOHN, V.S., RAJA, M., SU, Y.K., SEBASTIAN, P.J., Sol. Energy Mater. Sol. Cells, 88, 2005, p. 227.
12. SIMA, M., MANEA, A.C., SIMA, Ma., VISAN, T., Rev. Chim. (Bucharest), **58**, no. 8, 2007, p. 741.
13. SIMA, M., ENCULESCU, I., SIMA, Ma., VASILE, E., VISAN, T., Surf. Interf. Anal., 40, 2008, p. 651.
14. SIMA, Ma, VISAN, T., MATEI, E., UNGUREANU, F., ENCULESCU, I., SIMA, M., Z. Phys. Chem., 225, 2011, p. 325.
15. CHANDER, R., RAYCHAUDHURI, A.K., Solid State Commun., 145, 2008, p. 8.
16. PEULON, S., LINCOT, D., Adv. Mater., 8, 1996, p. 166.
17. SPEIGHT, J.G., Lange's Handbook of Chemistry, 16th ed, McGraw-Hill, New York, 2005, section 1.
18. SIMA, Ma, VASILE, E., SIMA, M., VISAN, T., Anal. Univ. Oradea – fasc. Chimie, 15, 2008, p. 98.
19. LIU, Z., JIN, Z., QIU, J., LIU, X., WU, W., LI, W., Semicond. Sci. Technol., 21, 2006, p. 60.
20. GANNE, F., CACHET, C., MAURIN, G., WIART, R., CHAUVEAU, E., PETITJEAN, J., J. Appl. Electrochem., 30, 2000, p. 665.
21. BAIK, D.S., FRAY, D.J., J. Appl. Electrochem., 31, 2001, p. 1141.
22. ZOLTOWSKI, P., J. Electroanal. Chem., 443, 1998, p. 149.
23. MACDONALD, J.R., Impedance Spectroscopy: Emphaizing Solid Materials and Analysis, J. Wiley & Sons, New York, 1987.
24. HOLZE, R., Electrochemical Thermodynamics and Kinetics, Springer, Berlin, 2007, p 342.
25. OGAWA, N., KIKUCHI, R., NAKAMURA, A., AIZAWA, H., IKEDA, S., Anal. Sci., 9, 1993, p. 847

Manuscript received: 18.12.2013